Large Density-Functional and Basis-Set Effects for the DMSO Reductase Catalyzed Oxo-Transfer Reaction

Li, Jilai; Mata, Ricardo A.; Ryde, Ulf

Published in:
Journal of Chemical Theory and Computation

DOI:
10.1021/ct301094r

2013

Large density-functional and basis-set effects for the DMSO reductase catalyzed oxo-transfer reaction

Ji-Lai Li†‡, Ricardo A. Mata§ and Ulf Ryde*†

Address:

†Department of Theoretical Chemistry, Lund University, Chemical Centre, P.O. Box 124, SE−221 00 Lund, Sweden

‡State Key Laboratory of Theoretical and Computational Chemistry, Institute of Theoretical Chemistry, Jilin University, Changchun 130023, People's Republic of China

§Institut für Physikalische Chemie, Georg-August-Universität Göttingen, Tammannstrasse 6, D-37077, Göttingen, Germany

* Corresponding author

E−mail: Ulf.Ryde@teokem.lu.se (UR)

Tel: +46−462224502

Fax: +46−462228648

Abstract
The oxygen-atom transfer reaction catalyzed by the mononuclear molybdenum enzyme dimethyl sulfoxide reductase (DMSOR) has attracted considerable attention by both experimental and theoretical studies. We show here that this reaction is more sensitive to details of quantum mechanical calculations that what has previously been appreciated. Basis sets of at least triple-zeta quality are needed to obtain qualitatively correct results. Dispersion has an appreciable effect on the reaction, in particular the binding of the substrate or the dissociation of the product (up to 34 kJ/mol). Polar and non-polar solvation effects are also significant, especially if the enzyme can avoid cavitation effects by using a pre-formed active-site cavity. Relativistic effects are considerable (up to 22 kJ/mol), but they are reasonably well treated by a relativistic effective core potential. Various density-functional methods give widely different results for the activation and reaction energy (differences of over 100 kJ/mol), mainly reflecting the amount of exact exchange in the functional, owing to the oxidation of Mo from +IV to +VI. By calibration towards local CCSD(T0) calculations, we show that none of eight tested functionals (TPSS, BP86, BLYP, B97-D, TPSSH, B3LYP, PBE0, and BHLYP) give accurate energies for all states in the reaction. Instead, B3LYP gives the best activation barrier, whereas pure functionals give more accurate energies for the other states. Our best results indicate that the enzyme follows a two-step associative reaction mechanism with an overall activation enthalpy of 63 kJ/mol, which is in excellent agreement with the experimental results.

Keywords: density functional calculations • reaction mechanism • oxygen-atom transfer • activation barrier • dispersion • non-polar solvation energy

TOC:

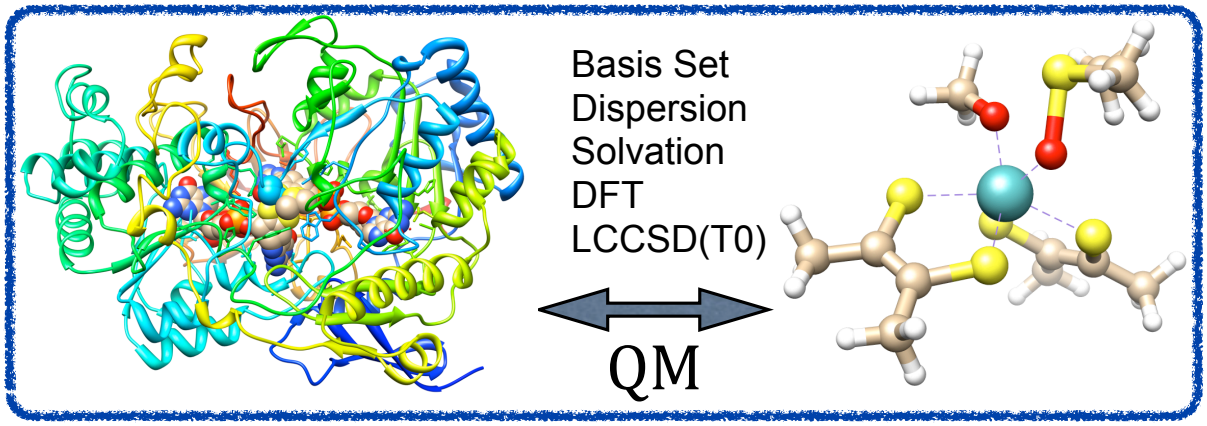

1. Introduction

The modeling of enzymatic reactions is fundamental to elucidate their catalytic mechanisms. In this area, quantum mechanical (QM) calculations have made major contributions because they can unravel enzymatic reaction mechanisms and provide detailed information on the energies, structures, and spectroscopic properties of relevant reactive species, in particular of transition states, which are hard to characterize with other methods. Thereby, they serve as a powerful tool in enzymology that is complementary to experimental analysis. However, the calculations are challenging with many potential sources of errors.

The dimethyl sulfoxide reductase (DMSOR) family is the largest and most diverse group of mononuclear molybdenum enzymes. DMSOR catalyzes the oxygen-atom transfer (OAT) from dimethyl sulfoxide (DMSO) to the Mo^{IV} active site, yielding dimethyl sulfide (DMS) and Mo^{VI}. Due to their biological and industrial relevance, OAT reactions involving high-valent oxo-Mo complexes have been extensively investigated,[1,2] including studies of inorganic models.[3,4] Available crystal structures of DMSOR show an active site in which Mo is coordinated to two molybdopterin molecules and one serine residue.[5] In the oxidized state, Mo binds an additional oxy group.[6]

Computational studies of DMSOR were pioneered by Webster and Hall,[7] performing B3LYP calculations on the model $[Mo(DMDT)_2(OCH_3)]^-$,[8] where DMDT is 1,2-dimethyldithiolene. They suggested an associative mechanism with an activation barrier of 37 kJ/mol for the S–O bond cleavage, starting from the Mo-bound DMSO complex. The corresponding transition-state structure was similar to the crystal structures of both the oxidized and reduced states, whereas the optimized product structure was quite different, indicating that DMSOR destabilizes the oxidized product state. This was confirmed by another combined B3LYP and PM3 study.[9] Thapper et al., studied a slightly different model system and obtained an activation barrier of 76 kJ/mol.[10] They optimized also the structure of the transition state for DMSO binding and showed that it was lower than that that for the S–O bond cleavage. These findings were confirmed also for the original model system by McNamara et al.,[11,12] Hernandez-Marin and Ziegler,[13] as well as Solomon et al.,[14,15] which obtained activation barriers of 80, 69, and 68 kJ/mol, respectively. The latter two groups have also explained the apparent conflict between theoretical calculations and kinetic experiments regarding the rate-limiting step of the reaction.[16] Hofmann demonstrated that density functional theory (DFT) methods and especially the B3LYP functional performed quite well for this reaction[17] and that all reactive species along the reaction coordinate were most stable in the singlet state.[18] However, they reported an activation barrier of only ~40 kJ/mol.

Despite the detailed understanding reached by these studies, we have found unexpectedly large changes in the calculated energies when the theoretical calculations are improved with larger basis sets, dispersion effects, non-polar solvation energies, and higher-level coupled cluster calculations. These results are described here, including comparisons with previous studies to explain the observed differences.

2. Computational Details

Throughout this article, we have used the QM cluster approach.[19] The active site of the reduced form of DMSOR was modeled by $[Mo(DMDT)_2(CH_3O)]^-$, where CH_3O^- is a model of the serine ligand. DMDT is a common model of the molybdopterin ligand, used in most previous theoretical studies[7,13-15,17,18] and also in kinetic experiments.[8] The starting coordinates were

obtained from available crystal structures.[5] For DMSO, several conformations are possible.[10] However, with our methods, they are close in energy, so we used the one observed in crystal structures of the protein, i.e. the same as in most previous calculations.[14] The DMSO substrate was explicitly modeled and was converted to DMS during the reaction. This model system is illustrated in Figure 1. To explore the effect of the net charge of the model, the counter ion Et_4N^+ from the inorganic models[8] was included in some calculations. In addition, test calculations were also performed in which the CH_3O^- ligand was replaced with PhO^-.

The DFT calculations were performed with the Turbomole 6.3[20] and ORCA[21] packages. The hybrid B3LYP density functional was employed in all calculations,[22,23] unless otherwise stated. It is the most widely used density functional and it has a well documented accuracy: For molecules containing first- and second-row atoms, the errors are seldom higher than 13 kJ/mol and for transition-metal biochemistry, the accuracy is normally within 21 kJ/mol.[19] In a previous study of the DMSOR reaction, B3LYP was deemed to be the most accurate functional among a selected set of DFT methods by comparison to CCSD benchmark values.[17] It has also been employed in most of the previous studies.[3,7,11,12,14,15,18]

Geometries were fully optimized without symmetry constraints. Harmonic vibrational frequencies were computed to verify the nature of the stationary points. Zero-point energies, as well as entropy and thermal corrections to the enthalpy and Gibbs free energy at 300 K and 1 atm pressure were obtained from the frequencies using an ideal-gas rigid-rotor harmonic-oscillator approximation. Such an approach has been successfully followed in other studies of enzyme reactions.[24,25]

If not otherwise stated, all structures were optimized with the def2-TZVPP basis set (denoted TZP in the following).[26] The density-fitting (resolution-of-the-identity approximation) and chain-of-sphere techniques, RIJCOSX,[27] were employed with the corresponding def2-TZVPP auxiliary basis set to accelerate the calculations at an insignificant loss in accuracy.[26] All geometry optimizations and energy calculations included DFT-D2 dispersion,[28] relativistic effects calculated with the zeroth-order regular approximation (ZORA),[29,30] and solvent effects obtained with the COSMO continuum-solvation model employing a dielectric constant of 4, a common choice to model a protein-like environment.[31] However, single-point energy calculations were also performed in a continuum solvent with a dielectric constant of 36 (acetonitrile) for the biomimetic inorganic model reaction and a dielectric constant of 78 for the DMSO substrate and DMS product in the enzyme reactions (these two molecules come from water solution). All COSMO calculations involved optimized radii of 1.30, 2.00, 1.72, 2.16, and 2.22, Å for H, C, O, S, and Mo, respectively. In all calculations, we used tight SCF convergence criteria and finer-than-default integration grids (Grid4 in ORCA) in order to get fully converged stationary points with accurate energies on the minimum-energy pathways.

In addition, non-polar continuum-solvation cavitation, dispersion, and repulsion energies were estimated for all complexes with the polarized continuum method (PCM)[32-34] as implemented in the Gaussian 03.[35] These calculations used the UAKS radii (united atom topological model for Kohn–Sham theory)[34] and they are needed to obtain valid solvation energies for all reactants, as well as a balance in the dispersion energy terms for reactions in which a ligand from solution binds to or dissociates from a metal complex.[36]

Single-point energy calculations were also performed with the def2-QZVPP (QZP) basis set.[26] The final reported energies include these basis-set corrections, the PCM corrections, as well as the zero-point vibrational energy (ZPE) and thermal corrections to the enthalpy, calculated on structures optimized at the B3LYP-D2/TZPP+ZORA+COSMO level of theory.

Test calculations were also performed with the def2-SVP (SVP) basis set, as well as with the DFT methods TPSS,[37] BP86,[38] BLYP,[39] B97-D,[28] TPSSH,[37,40] PBE0[41,42] and BHLYP[39,43], using the TZP basis set. These single-point energy calculations employed the MWB 28-electron relativistic effective core potential (ECP) for Mo instead of the ZORA treatment.[44]

In order to further refine the energetics of the reaction pathway, single-point calculations with local correlation methods were performed on the optimized structures. Due to the QM system size (with a triple-zeta quality basis set, the number of basis functions is close to 1000), canonical *ab initio* calculations would be extremely demanding. Local correlation alternatives allow for a reduction in computational cost and the treatment of such system sizes at a high-level of theory. We applied local coupled-cluster theory with single and double excitations and a non-iterative perturbative triples approximation (LCCSD(T0)).[45,46] All wavefunction calculations were performed with Molpro2010.1.[47] The LCCSD(T0) values were computed with the Dunning cc-pVTZ basis set[48] for all atoms except Mo, which was described with the aug-cc-pVTZ-PP orbital basis in combination with the Stuttgart/Dresden ECP28MDF pseudopotential[49] (this combination is called DTZ below). In order to correct for basis set incompleteness, second-order Møller–Plesset perturbation theory (MP2) calculations were carried out with the aug-cc-pVQZ basis (aug-cc-pVQZ-PP for Mo with the ECP28MDF pseudopotential).[48-50] The diffuse functions were removed for hydrogen atoms (this combination is called AQZ below). The final estimate for the electronic energy was obtained by combining the two results:

$$E_{CC} = E(\text{LCCSD(T0)/DTZ}) + E(\text{MP2/AQZ}) - E(\text{LMP2/DTZ}) \qquad (1)$$

The LMP2/DTZ energies are obtained in the local coupled cluster run. The use of the canonical MP2/AQZ energy also allows us to correct for the domain error (due to the truncation in the virtual space).[51] All wavefunction calculations were performed with density fitting approximations.[52-54] In the Hartree–Fock (HF) DTZ calculations, the Coulomb and exchange fitting basis sets used were def2-TZVPP for Mo and cc-pVTZ/JKFIT for all other atoms.[55,56] In the AQZ case, def2-QZVPP and aug-cc-pVQZ/JKFIT were used, respectively.[55,56] For the MP2 and LCCSD(T0) calculations, we used the cc-pVTZ/MP2FIT (def2-TZVPP MP2 for Mo) or aug-cc-pVQZ/MP2FIT (def2-QZVPP MP2 for Mo) fitting basis sets, respectively.[57,58]

The orbitals in the local correlation calculations were obtained through Pipek–Mezey localization.[59] The domains were determined according to the NPA criterion, with $T_{NPA} = 0.03$.[60] We have found in several studies that the latter threshold delivers more stable results than the Boughton–Pulay criterion, particularly with changes in the geometry or basis set. Test calculations were also performed with natural localized molecular orbitals, instead of Pipek–Mezey localization, but the difference was found to be small and not improving relative to canonical MP2 calculations.

In the LCCSD(T0) calculations, there are two main sources of error, viz. the domain and pair approximations. As mentioned above, the domain error is corrected by adding the difference between the canonical MP2/AQZ and LMP2/DTZ results. In the case of local coupled-cluster calculations, only near-lying occupied orbitals are fully included in the correlation treatment (those constituting so-called ‘strong pairs’). By default, orbitals separated by more than one bond are treated at the MP2 level, and only partly included in the triples calculation. We performed a series of tests to converge the results relative to these approximations. They will be discussed in the text below.

3. Results and Discussion

3.1 Structures

In this paper, we study the DMSOR reaction with the QM cluster approach, using a model system employed in several previous studies, $[Mo(DMDT)_2(CH_3O)]^-$.[7,14,15,18] We started by optimizing the separated substrate DMSO and the active-site model (SR). The latter was square pyramidal with the four S ligands in the square plane, as is shown in Figure 1. The Mo–S distances were 2.34–2.36 Å and the Mo–O_{Ser} distance was 1.86 Å (cf. Table 1; O_{Ser} is the O atom of the CH_3O^- model).

When DMSO was allowed to approach the Mo ion, an intermediate (IM) was found, characterized by a trigonal prismatic structure with DMSO *cis* to the CH_3O^- ligand and with a Mo–O_{DMSO} distance of 2.31 Å. The S_{DMSO}–O_{DMSO} bond is only 0.03 Å longer than in free DMSO, showing that it is still intact in this complex. Even if the Mo coordination number in the SR→IM step increases from five to six, the four S_{DMDT} atoms (S_1–S_4) remain in the square plane, as is shown by the S_1–S_2–S_3–S_4 dihedral angle, which is close to 180° in both structures (Table 1). IM is separated from SR by a transition state (TS1), which is characterized by a Mo–O_{DMSO} distance of 2.62 Å.

Subsequently, DMS can dissociate from the Mo complex, leaving a six-coordinate product complex $[MoO(DMDT)_2(CH_3O)]^-$ (SP), in which the Mo–O_{DMSO} bond is 1.71 Å, showing that it represents an oxy group. During this dissociation, a second transition state has to be passed (TS2), in which the S_{DMSO}–O_{DMSO} bond is elongated to 1.89 Å and Mo–O_{DMSO} bond has shortened to 1.91 Å. This shows that the S–O bond is cleaved and a Mo–O bond is formed in this step. In addition, the general structure of the Mo complex changes to a distorted octahedral structure, as is illustrated by a change in the S_1–S_2–S_3–S_4 dihedral angle from 176° in IM to 144° in TS2 and 103° in SP (cf. Figure 1).

The general structures of all these states are similar to those found in previous calculations of the DMSOR mechanism.[7,10-15,17,18] In particular, the importance of the trigonal prismatic structure has been emphasized,[61] as well as the fact that the enzyme seems to destabilize the product by avoiding a octahedral structure.[7] However, the Mo–O_{DMSO} distance in TS1 (2.62 Å) is appreciably shorter (indicating a later transition state) than in most previous calculations, 2.81–3.11 Å.[13]

3.2 Energies

The relative enthalpies of the various states are shown in Table 2 (ΔH column). The values are based on B3LYP calculations. It can be seen that IM lies 16 kJ/mol above the separated reactants (SR). TS1 is very close to IM in energy; with all energy corrections, its enthalpy is actually 1 kJ/mol below that of IM (further discussed below). On the other hand, TS2 is well separated from IM with a barrier of 56 kJ/mol (72 kJ/mol above SR). The separated products (SP) are 48 kJ/mol more stable than the separated reactants.

As mentioned in the method section, our calculated energies involve several corrections. These are also listed in Table 2. The geometries are optimized at the B3LYP-D2/TZP+ZORA+COSMO level (E_{opt} in Table 2), which gives a net activation barrier of 86 kJ/mol and 2 kJ/mol energy difference between TS1 and IM. To this energy, we add three corrections. The first is a basis-set correction (from the TZP to the QZP basis set). Quite satisfactorily, it is rather small, 4–9 kJ/mol. It is smaller for SP than for the other complexes,

indicating that it mainly corrects the basis-set superposition error. Second, there is a thermal correction to the enthalpy at 300 K and 1 atm pressure, obtained from the vibrational frequencies. It includes also the zero-point energy, which partly cancels the thermal effects. Together, they sum up to a quite small correction, –1 to 2 kJ/mol.

Third, we add the three non-polar continuum-solvation energy terms from PCM calculations (cavitation, dispersion, and repulsion energies, summed in Table 2). The repulsion energies are small (up to 2 kJ/mol) and negative. On the other hand, the dispersion and cavitation energies are large (59–197 kJ/mol), although they partly cancel – the dispersion provides a positive contribution of ~27 kJ/mol and the cavitation energy a negative contribution to the relative energies of the complexes (–63 kJ/mol). The reason for this is that in SR there are two separated molecules (DMSO and the $[Mo(DMDT)_2(OCH_3)]^-$ model), which interact with the surrounding solvent, whereas in TS1, IM, and TS2, they have formed a complex, thereby reducing the surface contact area in solution. This leads to a decrease in the dispersion and exchange-repulsion energies with the solvent, which is compensated by dispersion and exchange interactions within the complex. The latter are already included in E_{opt}. In fact, the intramolecular dispersion energy can be explicitly estimated from the DFT-D2 correction of the complexes – the results in Table 2 show that it is negative and more than counteract the solvation dispersion (–33 to –34 kJ/mol).

For the cavitation energy, we have used two estimates. The non-polar energies in brackets include all cavitation energies and apply primarily to the $[Mo(DMDT)_2(OCH_3)]^-$ model free in acetonitrile solution. The other one assumes that the cavitation energy of the enzyme model is constant throughout the reaction, i.e. that the enzyme active-site cavity does not change during the reaction and is not solvated before the substrate binds.[36] This seems to be a reasonable assumption, considering that the crystal structures of DMSOR show that the active site is buried in the enzyme.[5] From Table 2, it can be seen that the presence of a pre-formed cavity in the enzyme is predicted to give non-polar energies that favor the TS1, IM and TS2 states by 38 kJ/mol. For the inorganic model, the non-polar solvation energies add up to a small net effect of about –7 kJ/mol.

Table 2 also shows that the ZORA relativistic effects (which are included in E_{opt}) have a strong influence on the SP energy (–22 kJ/mol; owing to the change in the oxidation state of Mo), but smaller effects for the relative energies of the other states, –7 to 5 kJ/mol. Calculations with relativistic effects treated instead with the relativistic ECP in the Mo def2-TZVPP basis set give results that agree with ZORA within 3 kJ/mol (sum of the B3LYP data in Table 3 and the Solv energy in Table 2). COSMO polar solvation energies obtained for a protein-like dielectric constant of 4 were also included in E_{opt}. They amount to 6–15 kJ/mol. For the more polar acetonitrile solvent used in experiments with the $Mo(DMDT)_2$ model system, the effects are somewhat larger (7–22 kJ/mol, shown in brackets in Table 2). Moreover, for the enzyme reaction, DMSO and DMS come from aqueous solution, so we have added a correction for the difference in the polar solvation energy for these two molecules between a dielectric constant of 4 and 78 (water), which disfavors TS1, IM, and TS2 by 16 kJ/mol and SP by 11 kJ/mol (column SC in Table 2).

Finally, we have calculated the entropy correction, also allowing for calculations of free energies (*–TS* in Table 2). It can be seen that this correction is insignificant for SP, but large for the other three states, 57–63 kJ/mol. The latter term is completely dominated by the reduction in translational and rotational freedom when the two reactants form the complex. It has been argued that the simple Sackur–Tetrode equation used in these estimates overestimates this contribution in water solution by ~30 kJ/mol.[62-64] This is supported by the observation that our overall

activation entropy (i.e. $-TS$ of TS2), 63 kJ/mol, is 18 kJ/mol higher than the experimental estimate, 45 kJ/mol.[8]

Previous studies of DMSOR have typically included thermal, solvation, and relativistic effects obtained by Mo ECPs, as well as (when appropriate) entropy corrections. On the other hand, the basis-set, DFT-D, and non-polar solvation corrections have not been applied before. From Table 2, it can be seen that these corrections are substantial, reducing the relative energies of the TS1, IM, and TS2 states by 61–66 kJ/mol for the enzyme reaction. With this in mind, it is puzzling that the present results give an activation enthalpy (72 kJ/mol) that is similar or higher than that obtained in previous studies (38–80 kJ/mol). Therefore, we examined the effect of the basis sets and DFT functionals in the following two sections.

3.3 Effect of the basis sets

Previous studies have used varying basis sets, different from those used in this study, and in general smaller. Therefore, we run single-point energy calculations on our B3LYP-D2/TZP+ZORA+COSMO geometries using the smaller SVP basis set. From the results in Table 2 (E_{SVP} column), it can be seen that the smaller basis set gives energies that are very different from those obtained with the larger TZP basis set, with differences of up to 75 kJ/mol for TS2 and SP. With the smaller basis set, the energy difference between TS1 and IM increases to 11 kJ/mol and TS2 is only 12 kJ/mol above SR. Thus, using a too small basis set reduces the net activation energy by a similar amount of energy as the dispersion and non-polar solvation energies.

Similar results are obtained if the structures are optimized with the SVP basis set (Table S1 in the Supporting Information; the maximum energy difference between E_{opt} in Table 2 and E_{TZP} in Table S1 is 4 kJ/mol). However, the basis set has a significant effect on the calculated geometries: The Mo–O_{DMSO} distance in IM is shorter in the SVP structure (2.18 Å; cf. Table S2 in the SI) than in the TZP structure (2.31 Å). On the other hand, it is longer in TS1, 2.80 Å compared to 2.62 Å. The Mo–O_{DMSO} distances in the SVP structures are more similar to those reported in previous calculations (2.17–2.30 Å for IM and 2.81–3.11 Å for TS1).[5,8,65] The SVP basis set also predicts a somewhat earlier transition state for TS2, with a S_{DMSO}–O_{DMSO} distance of 1.84 Å (compared to 1.89 Å obtained with the TZP basis set), although the Mo–O_{DMSO} distances are nearly the same (1.92 and 1.91 Å).

3.4 Effect of the DFT functional

Previous studies have used either the B3LYP or BP86 DFT functionals. In fact, Hofmann has shown that the results depends quite strongly on the DFT functional used.[17] Therefore, we have recalculated the energies for the various states by single-point energies using eight different DFT functionals, BP86, TPSS, BLYP, B97-D, TPSSH, B3LYP, PBE0, and BHLYP. To make the energies comparable with each other and also with energies by other QM methods, they are pure DFT/QZP energies with the DFT-D3 correction (the DFT-D2 method is not parameterized for the TPSSH and BHLYP methods), but without any other corrections and with relativistic effects treated with the Mo ECP, instead of ZORA. From Table 3, it can be seen that all results for the TS1 and IM states are quite similar, with differences of up to 15 and 24 kJ/mol, respectively, BP86 or TPSS giving the lowest energy and B97-D the highest energy. However, for TS2, the energies vary extensively, from 23 kJ/mol for BP86 and TPSS to 139 kJ/mol for

BHLYP. The energy is small for the pure functionals and increases for the hybrid functionals, almost proportionally to the amount of Hartree–Fock exchange in the functional (10% for TPSSH, 20% for B3LYP, 25% for PBE0, and 50% for BHLYP). The variation is also large for SP, with the pure functionals giving more negative energies (–107 to –114 kJ/mol) than the hybrid functionals (–94 to –11 kJ/mol, again following the amount of Hartree–Fock exchange). This reflects that the oxidation state of the Mo ion has changed in SP and also partly in TS2, something that is frequently problematic to describe with the DFT functionals, giving a strong dependence on the amount of exact exchange of the functionals.[66,67]

To get an indication of which DFT functional gives the more reliable results, we estimated the electronic energies for the stationary structures with the LCCSD(T0) method (correcting for basis set incompleteness and domain errors with an MP2 correction as described in the Methods section). In the LCCSD(T0) calculations, the number of pairs included in the CCSD iterations (and the groups included in the triples list) are controlled by distance criteria.[45] In order to treat minima and transition states on an equal footing, it is necessary to control the effect of these approximations. They have been discussed in previous theoretical studies on enzymatic reactivity, in which the LCCSD(T0) method was applied to estimate reaction barrier heights.[68-70] In conformity with the previous studies, we found that a good convergence was obtained by including pairs separated by up to 3 Bohr (1.59 Å, between their domain centers) in the CCSD iterations, and building the triples list based on a close-pair distance of 5 Bohr (2.65 Å; $R_c = 3$, $R_w = 5$ as discussed in Ref. [70]). Furthermore, the LMP2 amplitudes of the latter pairs have been included in the CCSD residuals.[45]

One remaining question regarding the accuracy of the coupled-cluster treatment is the possible onset of multireference character along the reaction path. This could affect the triples correction, in particular. The norm of the $T1$ vector from the CCSD solutions did not give any indication of strong multireference effects. The values were relatively constant along the pathway, varying between 0.24 and 0.37. However, there are some alarming differences between LMP2, LCCSD, and LCCSD(T0), shown in Table 4. The differences in the relative energies of TS1 and IM are below 5 kJ/mol. This shows that the approach is robust for these states. However, the LMP2 result shows an error of ~100 kJ/mol for the relative energy of the SP state. The reason for this is again the change in oxidation state of Mo from Mo(IV) in SR to Mo(VI) in SP. Similar problems have been observed in other theoretical studies.[70,71] The triples correction is also relatively large (57 kJ/mol). It is therefore arguable whether LCCSD(T0) can provide a reliable estimate for the total reaction energy. However, we are mostly interested in the transition state TS2. In that case, the effect is much smaller than for the products, with an LMP2 error of 22 kJ/mol. This gives us some confidence on our approach to estimate the barrier height.

The local correlation results, including basis-set and domain corrections, which are also included in Table 3 (column E_{CC}, cf. Eqn. 1), show some interesting trends. For the relative energy of TS2, the E_{CC} result (67 kJ/mol) is most similar to that of the B3LYP method. On the other hand, for the other states, the E_{CC} results are closer to those of the BP86 and TPSS functionals (and also the BLYP and B97D functionals for PS; deviations of up to 9 kJ/mol), whereas the B3LYP results have errors of 16–32 kJ/mol. On average, TPSSH gives the best result with a mean absolute deviation (MAD) of 14 kJ/mol and a maximum error of 21 kJ/mol. On the other hand, the other functionals except BHLYP and PBE0 do not give much higher mean absolute errors (16–21 kJ/mol). In conclusion, these E_{CC} results indicate that B3LYP is accurate for the TS2 barrier, but it gives too high energies for the other states.

Hofmann has made a similar calibration of DFT functionals, using CCSD as a reference.[17] Unfortunately, he used a small basis sets (SVP quality) for the CCSD calculations, making the results less certain and forcing the authors to discard their CCSD(T) results as unrealistic (TS2 was below IM in energy). He concluded that B3LYP reproduces the CCSD results best among the DFT functionals, although the results show that B3LYP is best for TS2, whereas for the other states, pure functionals like BP86 perform better, exactly as in our investigation. Quantitatively, his results are unbalanced (e.g. giving a relative energy of 35 kJ/mol for TS2), owing to the use of a too small basis set (which leads to a strong underestimation of the correlation energy).

Finally, it should be noted that the DFT-D corrections are essential to get the DFT values close to the E_{CC} results – without these, the deviations increase for all methods and complexes except for SP, with MADs of 23–73 kJ/mol. This is expected, as the E_{CC} results include dispersion, in variance to the DFT methods. On the other hand, there is little difference between the results including the DFT-D2 and DFT-D3 corrections, less than 3 kJ/mol for B3LYP and TPSS, less than 5 kJ/mol for BLYP and PBE0, and up to 8–9 kJ/mol for BP86 and B97D.

3.5 Comparison with experiments

We can use the difference between the B3LYP and E_{CC} results as a method correction, which can be added to the energies in Table 2, yielding our final best estimates of the enthalpy and free energy for both the enzyme and model-system reactions shown in Figure 2. From this figure, it can be seen that we predict that the intermediate IM is 9 kJ/mol more stable than the separated reactants (SR). TS1 is 7 kJ/mol above IM, showing that this state reappears when the E_{CC} method correction is included (ΔH for TS1 is 1 kJ/mol below SR, but ΔG is 61 kJ/mol above it). Thus, our calculations suggest a two-step mechanism, in agreement with previous studies, which have given an energy difference between IM and TS1 of 4–24 kJ/mol. This barrier is small and therefore sensitive to details in the calculations. In fact, in previous calculations of a $[Mo(S_2C_2H_2)_2(PhO)]^-$ model, neither TS1 nor IM were found, indicating a single-step mechanism.[13]

For the activation enthalpy, our best estimate is 63 kJ/mol for the enzyme reaction and 83 kJ/mol for the model system. The former is in excellent agreement with the estimated enthalpy of activation for the enzyme of 63 kJ/mol.[72] On the other hand, the estimate for the inorganic model is somewhat higher than what has been experimentally estimated for the biomimetic model $[Mo(DMDT)_2(PhO)]^-$, 62 kJ/mol in acetonitrile.[8] The difference is perhaps a little bit larger than what can be expected from this type of calculations, especially for a pure inorganic model, where the continuum solvation approach can be expected to be quite accurate (the solvent is homogeneous, there are no doubt that the full cavitation energies should be included, and there is no problematic association entropy).

To study this reaction somewhat further, we introduced Et_4N^+, used as the counter ion in the biomimetic experiments. However, as can be seen in Table S3, this had only a small effect on the calculated energies, up to 8 kJ/mol. In particular, the activation barrier for TS2 is reduced by only 2 kJ/mol.

Moreover, the experimental results were obtained with a PhO^- ligand, rather than the CH_3O^- group used in our calculations. Therefore, we also performed calculations on the $[MoO(DMDT)(PhO)]^-$ model. Interestingly, the results in Table 5 show that the PhO^- model gives a lower TS2 activation barrier than the CH_3O^- group, by 8 kJ/mol for the E_{opt} energy (note that the E_{opt} results in Table 5 were obtained in a COSMO continuum solvent with $\varepsilon = 36$, so that it should be compared to E_{opt} + Solv(ε=36) – Solv(ε=4) in Table 2) and by 12 kJ/mol the fully

LCCSD(T0)-corrected enthalpy (ΔH = 71 kJ/mol in Table 5). This is reasonably close to the experimental estimate (63 kJ/mol[72]). Previous theoretical calculations obtained slightly smaller activation-energy difference between PhO^- and CH_3O^-, 5 kJ/mol),[13] but they did not find the IM and TS1 states, in contrast to our calculations. Thus, our results indicate that both the enzyme and the model-system reactions should follow a two-step mechanism. The geometries of all states (Table S4) are similar to those obtained with the CH_3O^- model, except that the Mo–O_{DMSO} distance is appreciably longer in TS1 (2.95, compared to 2.62 Å) and the S_1–S_2–S_3–S_4 dihedral angles are appreciably smaller in the TS1 and IM states (158 and 163°, compared to 178 and 176°).

Finally, it interesting to note that all previous theoretical calculations have given similar results for the activation enthalpy, 38–80 kJ/mol,[3,4] although important energy terms have been missing. In fact, these results have been obtained either with the BP86 method with a TZP basis set or with B3LYP method with a too small basis set. Our results in Tables 2 and 3 show that both approaches give a 50–80 kJ/mol too low barrier. However, these deficiencies are compensated by the missing dispersion and non-polar solvation effects, leading to an activation enthalpy in agreement with the experimental result, although for the wrong reason. This illustrates the danger of accepting a result close to experimental data without checking that the calculations are converged with respect to the basis set and theoretical methods used.

4. Conclusions

In this paper, we have studied the oxygen-atom transfer from DMSO to active-site models of DMSO reductase with computational methods. Our results show that DMSOR follows a two-step associative mechanism with the binding of DMSO in the first step, and the oxygen-atom transfer and dissociation of the DMS product in the second step. The first transition state is close in energy to the intermediate (within ~10 kJ/mol), whereas the rate-limiting barrier is observed for the second step. We obtain activation enthalpies in excellent agreement with experiments for both the enzyme reaction (63 compared to 63 kJ/mol) and an inorganic model system (71 compared to 62 kJ/mol), but in the latter case only if a full $[Mo(DMDT)_2(PhO)]^-$ model is considered.

We show that this reaction is unexpectedly sensitive to details in the calculations. First, increasing the basis sets from SVP to TZP changes the relative energies by up to 75 kJ/mol, showing that results obtained with the smaller basis set are completely useless. Further increasing the basis set to QZP has a smaller effect on the energies (4–12 kJ/mol).

Second, different DFT functionals give results that vary by up to 116 kJ/mol. We show that the large effects are restricted to the TS2 and SP states, and that they reflect the amount of Hartree–Fock exchange in the methods. This is quite expected, because similar effects have been observed before for energy differences between different spin states,[73] as well as between different oxidation states of transition metals[66,67] (in SP and partly in TS2, Mo is oxidized from Mo(IV) to Mo(VI)). By calibration to LCCSD(T0) calculations with basis-set and domain corrections (E_{CC} in Eqn. 1), we show that B3LYP gives the most accurate result for TS2, whereas for the other states, the pure TPSS and BP86 functionals give the more accurate results. Thus, there is no single DFT functional that gives accurate results for all five states. Instead, we employ a method correction (B3LYP→E_{CC}) for all states. This also shows that LCCSD(T0) is a powerful method for routine calculations on realistic model systems of biochemical reactions.

Third, we show that dispersion and non-polar solvation corrections, which have not been considered before, are also crucial for accurate reaction energies. The DFT-D internal dispersion

corrections stabilize the intermediate states (TS1, IM1, and TS2) by ~33 kJ/mol. Likewise, the non-polar solvation energies (cavitation, dispersion, and repulsion energies with the surrounding solvent) increase the stability of the intermediate states with another 7 kJ/mol. For an enzyme reaction, a pre-formed active site cavity can decrease the cavitation energy, which could further increase the stability of the intermediate state by up to 32 kJ/mol. This shows that for the enzyme reaction, the treatment of solvation effects is as crucial for the accuracy as the theoretical method and basis set. For more accurate results, QM/MM methods are needed and we have recently started such a project.

Quite amazingly, these results are in quantitative agreement with previous theoretical studies,[7,10-15,17,18,61] in spite of our significant improvements in the theoretical method. The reason for this is that errors in the DFT functionals or basis sets used in the previous studies have been compensated by errors caused by the missing dispersion and non-polar solvation effects.

Acknowledgements
This work has been supported by grants from the Swedish research council (Project 2010−5025) and the Crafoord foundation, as well as by computer resources of Lunarc at Lund University. Support from the Deutsche Forschungsgemeinschaft (International Research Training Group GRK 1422 "Metal Sites in Biomolecules: Structures, Regulation and Mechanisms"; see www.biometals.eu) is acknowledged. This work has also received support by the National Basic Research Program of China (973 Program) (2012CB932800), National Natural Science Foundation of China (NSFC 21103064, 21073075), the Special Funding of State Key Laboratory of Theoretical and Computational Chemistry, Jilin University.

Supporting Information
Energies and geometries obtained with calculations using the SVP basis set, energies obtained with the Et_4N^+ counter ion, and geometries obtained with the $[Mo(DMDT)_2(PhO)]^-$ model system. This information is available free of charge via the Internet at http://pubs.acs.org/.

References
(1) Enemark, J. H.; Cooney, J. J.; Wang, J. J.; Holm, R. H. *Chem. Rev.* **2004**, *104*, 1175.
(2) Hille, R. *Chem. Rev.* **1996**, *96*, 2757.
(3) Metz, S.; Thiel, W. *Coord. Chem. Rev.* **2011**, *255*, 1085.
(4) Holm, R. H.; Solomon, E. I.; Majumdar, A.; Tenderholt, A. *Coord. Chem. Rev.* **2011**, *255*, 993.
(5) Li, H. K.; Temple, C.; Rajagopalan, K. V.; Schindelin, H. *J. Am. Chem. Soc.* **2000**, *122*, 7673.
(6) McAlpine, A. S.; McEwan, A. G.; Bailey, S. *J. Mol. Biol.* **1998**, *275*, 613.
(7) Webster, C. E.; Hall, M. B. *J. Am. Chem. Soc.* **2001**, *123*, 5820.
(8) Lim, B. S.; Sung, K. M.; Holm, R. H. *J. Am. Chem. Soc.* **2000**, *122*, 7410.
(9) Mohr, M.; McNamara, J. P.; Wang, H.; Rajeev, S. A.; Ge, J.; Morgado, C. A.; Hillier, I. H. *Faraday Discuss.* **2003**, *124*, 413.
(10) Thapper, A.; Deeth, R. J.; Nordlander, E. *Inorg. Chem.* **2002**, *41*, 6695.
(11) McNamara, J. P.; Hillier, I. H.; Bhachu, T. S.; Garner, C. D. *Dalton Trans.* **2005**, 3572.
(12) McNamara, J. P.; Joule, J. A.; Hillier, I. H.; Garner, C. D. *Chem. Commun.* **2005**, 177.
(13) Hernandez-Marin, E.; Ziegler, T. *Can. J. Chem.* **2010**, *88*, 683.

(14) Tenderholt, A. L.; Wang, J. J.; Szilagyi, R. K.; Holm, R. H.; Hodgson, K. O.; Hedman, B.; Solomon, E. I. *J. Am. Chem. Soc.* **2010**, *132*, 8359.
(15) Tenderholt, A. L.; Hodgson, K. O.; Hedman, B.; Holm, R. H.; Solomon, E. I. *Inorg. Chem.* **2012**, *51*, 3436.
(16) Sung, K. M.; Holm, R. H. *J. Am. Chem. Soc.* **2002**, *124*, 4312.
(17) Hofmann, M. *J. Mol. Struc-Theochem.* **2006**, *773*, 59.
(18) Hofmann, M. *Inorg. Chem.* **2008**, *47*, 5546.
(19) Siegbahn, P. E.; Borowski, T. *Acc. Chem. Res.* **2006**, *39*, 729.
(20) TURBOMOLE V6.3 2011, a development of University of Karlsruhe and Forschungszentrum Karlsruhe GmbH, 1989-2007, TURBOMOLE GmbH, since 2007; available from http://www.turbomole.com. **2011**.
(21) Neese, F. ORCA -An Ab Initio, Density Functional and Semiempirical Program Package 2010, version 2.8; Bonn University: Germany, **2010**.
(22) Becke, A. D. *J. Chem. Phys.* **1993**, *98*, 5648.
(23) Kim, K.; Jordan, K. D. *J. Phys. Chem.* **1994**, *98*, 10089.
(24) Senn, H. M.; Thiel, W. *Angew. Chem. Int. Ed.* **2009**, *48*, 1198.
(25) Siegbahn, P. E. M.; Himo, F. *WIREs Comput. Mol. Sci.* **2011**, *1*, 323.
(26) Weigend, F.; Ahlrichs, R. *Phys. Chem. Chem. Phys.* **2005**, *7*, 3297.
(27) Neese, F.; Wennmohs, F.; Hansen, A.; Becker, U. *Chem. Phys.* **2009**, *356*, 98.
(28) Grimme, S. *J. Comput. Chem.***2006**, *27*, 1787.
(29) Lenthe, E. v.; Baerends, E. J.; Snijders, J. G. *J. Chem. Phys.* **1993**, *99*.
(30) van Wullen, C. *J. Chem. Phys.* **1998**, *109*, 392.
(31) Klamt, A.; Schüürmann, G. *J. Chem. Soc., Perkin Trans.* **1993**, *2*, 799.
(32) Cossi, M.; Tomasi, J.; Cammi, R. *Int. J. Quantum Chem.* **1995**, *56*, 695.
(33) Miertus, S.; Scrocco, E.; Tomasi, J. *Chem. Phys.* **1981**, *55*, 117.
(34) Tomasi, J.; Mennucci, B.; Cammi, R. *Chem. Rev.* **2005**, *105*, 2999.
(35) Gaussian 03, Revision E01; M. J. Frisch, G. W. T., H. B. Schlegel, G. E. Scuseria,; M. A. Robb, J. R. C., J. A. Montgomery, Jr., T. Vreven,; K. N. Kudin, J. C. B., J. M. Millam, S. S. Iyengar, J. Tomasi,; V. Barone, B. M., M. Cossi, G. Scalmani, N. Rega,; G. A. Petersson, H. N., M. Hada, M. Ehara, K. Toyota,; R. Fukuda, J. H., M. Ishida, T. Nakajima, Y. Honda, O. Kitao,; H. Nakai, M. K., X. Li, J. E. Knox, H. P. Hratchian, J. B. Cross,; V. Bakken, C. A., J. Jaramillo, R. Gomperts, R. E. Stratmann,; O. Yazyev, A. J. A., R. Cammi, C. Pomelli, J. W. Ochterski,; P. Y. Ayala, K. M., G. A. Voth, P. Salvador, J. J. Dannenberg,; V. G. Zakrzewski, S. D., A. D. Daniels, M. C. Strain,; O. Farkas, D. K. M., A. D. Rabuck, K. Raghavachari,; J. B. Foresman, J. V. O., Q. Cui, A. G. Baboul, S. Clifford,; J. Cioslowski, B. B. S., G. Liu, A. Liashenko, P. Piskorz,; I. Komaromi, R. L. M., D. J. Fox, T. Keith, M. A. Al-Laham,; C. Y. Peng, A. N., M. Challacombe, P. M. W. Gill,; B. Johnson, W. C., M. W. Wong, C. Gonzalez, and J. A. Pople,; Gaussian, I., Wallingford CT, 2004.
(36) Ryde, U.; Mata, R. A.; Grimme, S. *Dalton Trans.* **2011**, *40*, 11176.
(37) Tao, J.; Perdew, J. P.; Staroverov, V. N.; Scuseria, G. E. *Phys. Rev. Lett.* **2003**, *91*, 146401.
(38) Perdew., J. P. *Phys. Rev. B* **1986**, *33*, 8822.
(39) Lee, C.; Yang, W.; Parr, R. G. *Phys. Rev. B* **1988**, *37*, 785.
(40) Staroverov, V. N.; Scuseria, G. E.; Tao, J. M.; Perdew, J. P. *J. Chem. Phys.* **2003**, *119*, 12129.
(41) Perdew, J. P.; Burke, K.; Ernzerhof, M. *Phys. Rev. Lett.***1996**, *77*, 3865.

(42) Perdew, J. P.; Emzerhof, M.; Burke, K. *J. Chem. Phys.* **1996**, *105*, 9982.
(43) Becke, A. D. *J. Chem. Phys.* **1993**, *98*, 1372.
(44) Andrae, D.; Haeussermann, U.; M. Dolg, H. S.; Preuss, H. *Theor. Chim. Acta* **1990**, *77*, 123.
(45) Hampel, C.; Werner, H.-J. *J. Chem. Phys.* **1996**, *104*, 6286.
(46) Werner, H. J.; Schutz, M. *J. Chem. Phys.* **2011**, *135*, 144116.
(47) MOLPRO, a package of ab initio programs, version 2010; H.-J. Werner, P. J. Knowles, G. Knizia, F. R. Manby, M. Schütz et al., **2010**.
(48) Dunning, T. H. *J. Chem. Phys.* **1989**, *90*, 1007.
(49) Peterson, K. A.; Figgen, D.; Dolg, M.; Stoll, H. *J. Chem. Phys.* **2007**, *126*, 124101.
(50) Kendall, R. A.; Dunning, T. H.; Harrison, R. J. *J. Chem. Phys.* **1992**, *96*, 6796.
(51) Mata, R. A.; Werner, H. J. *J. Chem. Phys.* **2006**, *125*, 184110.
(52) Schutz, M.; Werner, H. J.; Lindh, R.; Manby, F. R. *J. Chem. Phys.* **2004**, *121*, 737.
(53) Werner, H.-J.; Manby, F. R.; Knowles, P. J. *J. Chem. Phys.* **2003**, *118*, 8149.
(54) Polly, R.; Werner, H. J.; Manby, F. R.; Knowles, P. J. *Mol. Phys.* **2004**, *102*, 2311.
(55) Weigend, F. *J. Comput. Chem.***2008**, *29*, 167.
(56) Weigend, F. *Phys. Chem. Chem. Phys* **2002**, *4*, 4285.
(57) Hellweg, A.; Hattig, C.; Hofener, S.; Klopper, W. *Theor. Chem. Acc.* **2007**, *117*, 587.
(58) Weigend, F.; Kohn, A.; Hattig, C. *J. Chem. Phys.* **2002**, *116*, 3175.
(59) Pipek, J.; Mezey, P. G. *J. Chem. Phys.* **1989**, *90*, 4916.
(60) Mata, R. A.; Werner, H. J. *Mol. Phys.* **2007**, *105*, 2753.
(61) Kaupp, M. *Angew. Chem. Int. Ed.* **2004**, *43*, 546.
(62) Irudayam, S. J.; Henchman, R. H. *J. Phys. Chem. B* **2009**, *113*, 5871.
(63) Dunitz, J. D. *Science* **1994**, *264*, 670.
(64) Rulisek, L.; Jensen, K. P.; Lundgren, K.; Ryde, U. *J. Comput. Chem.* **2006**, *27*, 1398.
(65) George, G. N.; Hilton, J.; Rajagopalan, K. V. *J. Am. Chem. Soc.* **1996**, *118*, 1113.
(66) Heimdal, J.; Kaukonen, M.; Srnec, M.; Rulisek, L.; Ryde, U. *Chemphyschem* **2011**, *12*, 3337.
(67) Jensen, K. P.; Ryde, U. *J. Phys. Chem. A* **2003**, *107*, 7539.
(68) Claeyssens, F.; Harvey, J. N.; Manby, F. R.; Mata, R. A.; Mulholland, A. J.; Ranaghan, K. E.; Schutz, M.; Thiel, S.; Thiel, W.; Werner, H. J. *Angew. Chem. Int. Ed.* **2006**, *45*, 6856.
(69) Mata, R. A.; Werner, H. J.; Thiel, S.; Thiel, W. *J. Chem. Phys.* **2008**, *128*, 025104.
(70) Dieterich, J. M.; Werner, H. J.; Mata, R. A.; Metz, S.; Thiel, W. *J. Chem. Phys.* **2010**, *132*, 035101.
(71) Ilich, P.; Hille, R. *J. Am. Chem. Soc.* **2002**, *124*, 6796.
(72) Cobb, N.; Conrads, T.; Hille, R. *J. Biol. Chem.* **2005**, *280*, 11007.
(73) Reiher, M.; Salomon, O.; Artur Hess, B. *Theor. Chem. Acc.* **2001**, *107*, 48.
(74) Bray, R. C.; Adams, B.; Smith, A. T.; Richards, R. L.; Lowe, D. J.; Bailey, S. *Biochem.* **2001**, *40*, 9810.

Figure 1. Structures of the various states along DMSOR reaction obtained at the B3LYP-D2/TZP+ZORA+COSMO level. Key geometry parameters are given in Table 1.

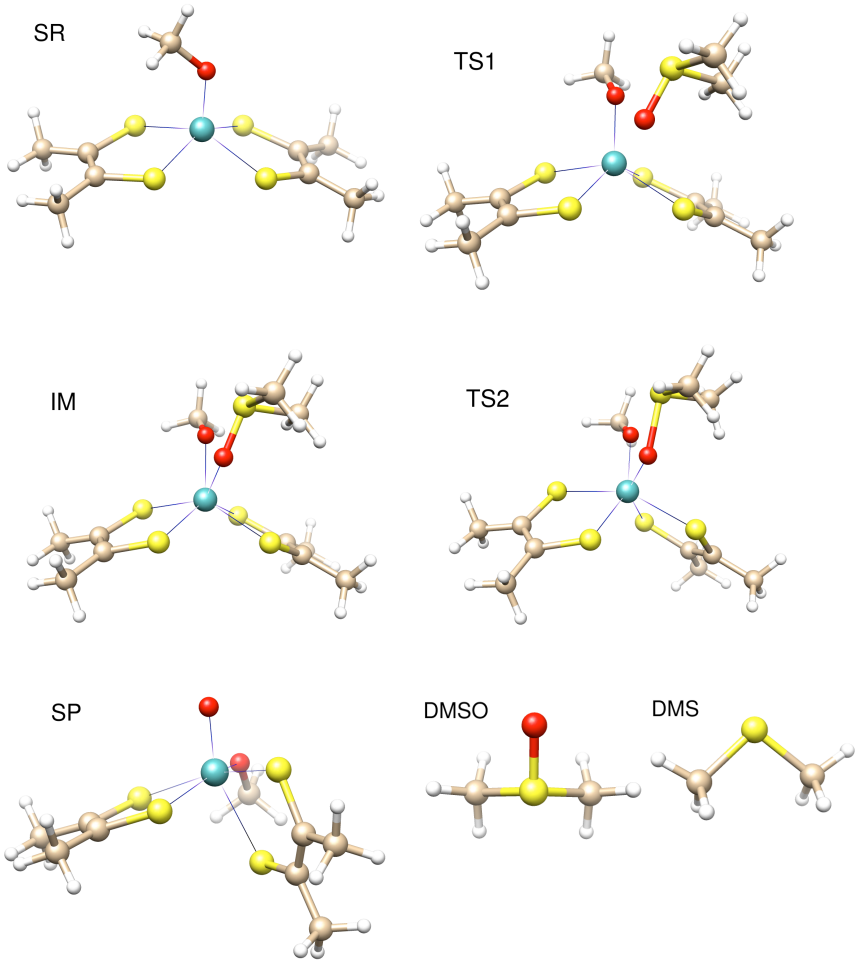

Figure 2. Final calculated energies for the oxo transfer from Me_2SO to $[Mo(OMe)(DMDT)^{2}]^{-}$. The enthalpies and Gibbs free energies with all corrections are given in black, magenta, blue and red, respectively. The energies are obtained from the data in Table 2 with the method correction added (the difference in energy between LCCSD(T0) and B3LYP from Table 3), but excluding the basis-set correction.

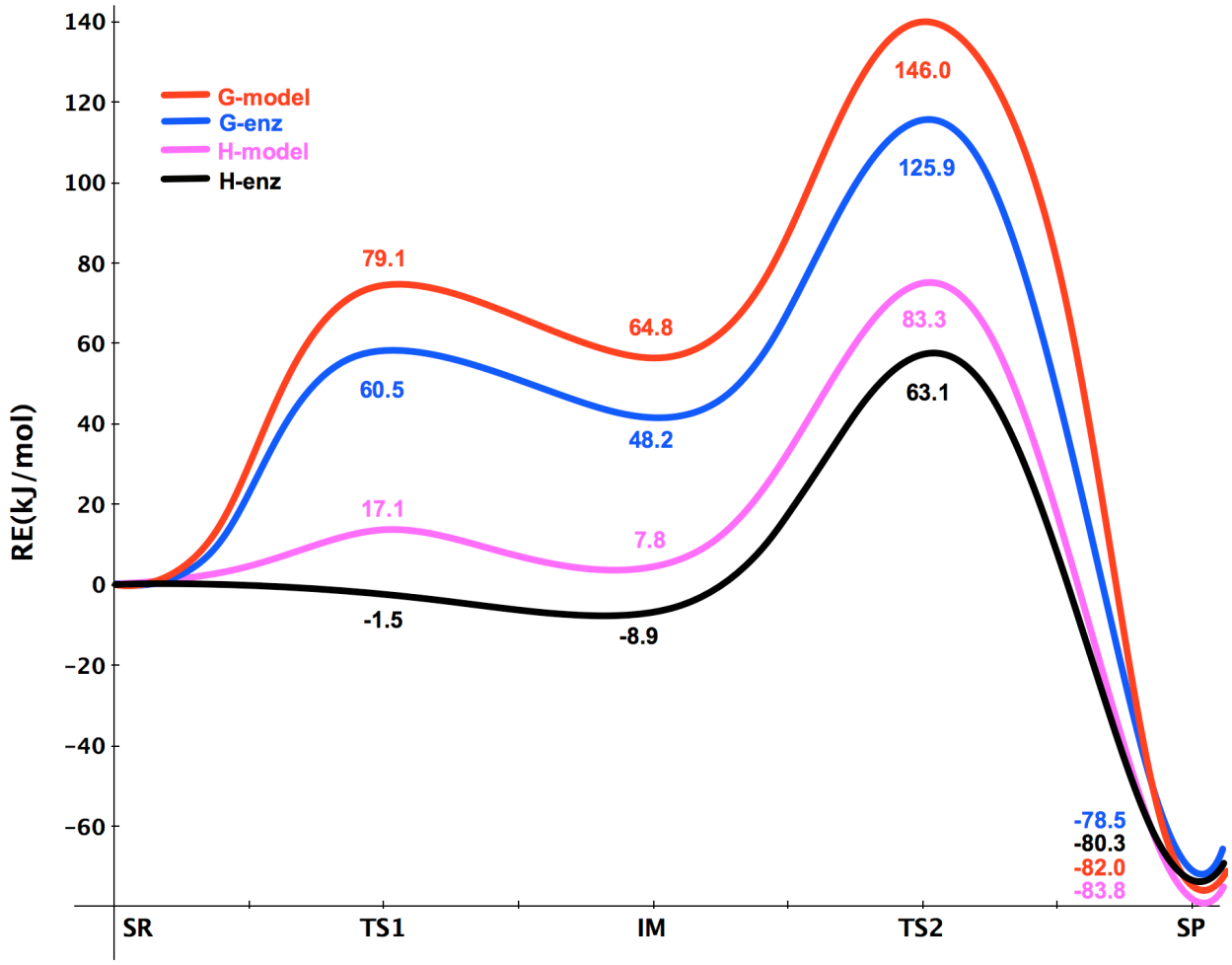

Table 1. Important distances, angles, and dihedral angles in the various states of the DMSOR reaction, obtained at the B3LYP-D2/TZP+ZORA+COSMO level, together with selected X-ray crystal data (PDB structures 1H5N[74] and 4DMR[6]).[a]

	$Mo–O_D$	$Mo–O_{Ser}$	$Mo–S_1$	$Mo–S_2$	$Mo–S_3$	$Mo–S_4$	$O_D–S_D$	MoO_DS_D	S_2MoS_3	$S_1S_2S_3S_4$
SR		1.86	2.34	2.34	2.36	2.36	1.50		144.1	180.2
TS1	2.62	1.94	2.37	2.35	2.36	2.38	1.51	116.6	140.1	177.6
IM	2.31	1.99	2.38	2.37	2.37	2.39	1.53	121.4	140.2	175.5
TS2	1.91	1.99	2.43	2.42	2.42	2.44	1.89	121.3	151.5	143.7
SP	1.71	1.94	2.45	2.43	2.61	2.42			158.1	102.8
1H5N		1.88	2.34	2.38	2.42	2.30			151.2	153.9
4DMR	2.25	2.03	2.37	2.41	2.45	2.34	1.54	120.4	148.1	155.0

[a] S_1 and S_2 are the two S atoms of one of the DMDT ligands, whereas S_3 and S_4 are the two S atoms of the other DMDT ligand. In the five-coordinate complexes, S_1 and S_4 are trans to each other. O_D and S_D are the O and S atoms of DMSO.

Table 2. The various energy components and corrections (kJ/mol) for the various states of the DMSOR reaction.

State	E_{opt}[a]	Basis[b]	H_{therm}[c]	Non-pol[d]	SC[e]	$-TS$[f]	DFT-D2[g]	ZORA[h]	Solv[i]	ΔH[j]	E_{SVP}[k]
SR	0.0	0.0	0.0	0.0	0.0	0.0	0.0	0.0	0.0	0.0	0.0
TS1	30.6	6.7	0.1	-38.3(-6.2)	15.8	62.0	-34.2	5.3	7.8(10.1)	14.9 (33.4)	1.0
IM	28.9	7.3	2.1	-37.9(-6.8)	15.8	57.0	-32.9	5.5	6.0(7.3)	16.2 (32.9)	-10.0
TS2	86.1	8.9	-0.9	-37.5(-6.9)	15.8	62.7	-32.6	-7.0	14.6(19.9)	72.3 (93.5)	12.1
SP	-62.6	3.8	-0.7	0.0(0.0)	11.1	1.8	-6.8	-22.1	14.5(22.0)	-48.5 (-52.0)	-137.7

[a] The uncorrected QM energy, obtained from the geometry optimizations (B3LYP-D2/TZP+ZORA+COSMO level)
[b] The basis-set correction (from TZP to QZP).
[c] The thermal enthalpy correction including the zero-point energy.
[d] The sum of the three PCM non-polar continuum solvation energy corrections (cavitation, dispersion, and repulsion).[l]
[e] A solvent correction for the difference in polar solvation energy of DMSO and DMS between a dielectric constant (ε) of 4 and 78.
[f] The entropy contribution (at 300 K; can be used to obtain free energies).
[g] The DFT-D2 dispersion correction.[m]
[h] The ZORA relativistic energy correction.[m]
[i] The COSMO electrostatic solvation energy.[l,m]
[j] The enthalpy at 300 K. For the enzyme reaction, $\Delta H = E_{opt}$ + basis + H_{therm} + Non-pol (enzyme[l]) + SC, whereas for the model complexes, $\Delta H = E_{opt}$ + basis + H_{therm} + Non-pol (model[l]) + Solv(ε=36) – Solv(ε=4).[l]
[k] The single-point B3LYP-D2/SVP+ZORA+COSMO energies calculated on the TZP geometries.
[l] When two values are given, the first applies to an enzyme reaction (constant cavitation energies and ε = 4 for the Mo models, but full PCM cavitation energies and ε = 78 for DMSO and DMS), whereas the one in brackets applies for the $[Mo(DMDT)_2(OCH_3)]^-$ model complex (including cavitation energies for all reactants and solvation energies calculated with ε = 36, acetonitrile).
[m] Note that the DFT-D2, ZORA, and Solv corrections are included in E_{opt} and they are obtained from single-point QM calculations where the corrections have been turned off.

Table 3. Energies for the various states in the DMSOR reaction (kJ/mol) obtained by single-point energy calculations with various methods on the B3LYP-D2/TZP+ZORA+COSMO geometries.[a]

State	BP86	TPSS	BLYP	B97D	TPSSH	B3LYP	PBE0	BHLYP	E_{CC}
SR	0.0	0.0	0.0	0.0	0.0	0.0	0.0	0.0	0.0
TS1	14.3	16.9	24.8	29.2	18.3	25.9	23.4	28.0	9.5
IM	13.1	11.5	27.6	35.3	13.4	27.4	21.6	28.0	2.4
TS2	23.3	23.2	33.5	50.2	46.1	76.6	86.6	139.1	67.4
SP	-103.1	-112.4	-113.7	-106.6	-94.0	-75.9	-53.1	-10.9	-107.8
MAD	16.1	16.3	20.1	17.7	13.7	20.6	26.7	53.2	0

[a] All energies are uncorrected, besides that the eight DFT energies include a DFT-D3 correction. The DFT results were obtained with the QZP basis set and Turbomole software (without ZORA or solvation, but with a relativistic ECP for Mo). The LCCSD(T0) composite results (E_{CC}) are described in Eqn. 1. MAD is the mean absolute difference in the relative energies (disregarding the SR state) compared to the E_{CC} results.

Table 4. Energies for the DMSOR reaction (kJ/mol) obtained by local correlation methods with the DTZ basis on the B3LYP-D2/TZP+ZORA+COSMO geometries.[a]

State	LMP2	LCCSD	LCCSD(T0)
SR	0.0	0.0	0.0
TS1	15.8	24.0	20.9
IM	10.8	20.2	16.2
TS2	97.0	105.5	75.4
SP	-254.2	-78.8	-136.2

[a] All energies are uncorrected.

Table 5. Relative electronic energies (kJ/mol) of the OAT reaction between DMSO and $[Mo(DMDT)_2(PhO)]^-$ (with a PhO^- instead of the CH_3O^- group).[a]

State	E_{opt}	Basis	H_{therm}	Non-pol	B3LYP+D3	E_{CC}	ΔH
SR	0.0	0.0	0.0	0.0	0.0	0.0	0.0
TS1*	31.9	12.5	-5.1	2.8	21.6	17.3	25.3
IM	22.8	10.8	-2.1	1.0	20.3	0.2	1.6
TS2	83.1	13.5	-3.4	-0.5	65.6	57.6	71.4
SP	-56.6	5.1	-3.3	0.8	-80.4	-107.8	-86.6

[a] The geometries were optimized with the B3LYP+D2/TZP+ZORA+COSMO method and energies were obtained with the B3LYP+D3/TZP(Mo ECP) and LCCSD(T0) methods (always with a dielectric constant of 36). $\Delta H = E_{opt} + H_{therm} + E_{CC} -$ B3LYP+D3. The other columns have the same meaning as in Table 2.